Journal of Alloys and Compounds 502 (2010) 371–375

Contents lists available at ScienceDirect

Journal of Alloys and Compounds

journal homepage: www.elsevier.com/locate/jallcom

Preparation of Ni-precipitated hBN powder by rotary chemical vapor deposition and its consolidation by spark plasma sintering

Jianfeng Zhang, Rong Tu, Takashi Goto*

Institute for Materials Research, Tohoku University, Sendai 980-8577, Japan

ARTICLE INFO

Article history:
Received 26 February 2010
Received in revised form 9 April 2010
Accepted 24 April 2010
Available online 4 May 2010

Keywords:
Rotary chemical vapor deposition (RCVD)
Hexagonal boron nitride (hBN)
Ni
Spark plasma sintering (SPS)

ABSTRACT

Ni nanoparticles were uniformly precipitated on hBN powder by rotary chemical vapor deposition (RCVD) using nickelocene ($NiCp_2$) as a precursor. The average grain size and the content of Ni increased from 13.9 to 84.5 nm and 0.98 to 3.65 mass%, respectively, with increasing supply rate (R_s) of $NiCp_2$ from 0 to 1.12×10^{-6} kg s^{-1}. The Ni-precipitated hBN powder was consolidated by spark plasma sintering. The density of the hBN body increased with increasing Ni content and sintering temperature. The highest density was 97.3% at 2273 K.

1. Introduction

Boron nitride (hBN) has several poly-types, typically hexagonal BN (hBN) and cubic BN (cBN). In particular, hBN is characterized by high-temperature refractoriness, chemical inertness, high lubrication, excellent thermal shock resistance and extremely low electrical conductivity [1,2]. Thus, hBN has been widely applied as insulators for high-temperature furnaces, protective tubes and insulating sleeves of thermocouples, crucibles, boats and nozzles for molten metals. Pressureless sintering, hot pressing and hot isostatic pressing have been applied for the preparation of hBN [1–5]; however, the densification of hBN is rather difficult due to its strong covalent bonding nature and anistrophic plate-like structure. In the sintering process, a small amount of boron oxide (B_2O_3) has been commonly added to densify hBN powder by liquid sintering [2]. However, B_2O_3 often deteriorates the water-resistance and high-temperature properties of hBN.

A small amount of metals would be an effective sintering additive, e.g., Al_2O_3/Ni [6], Al_2O_3/Cr [7], ZrO_2/Mo [8,9] and AlN/Mo [10,11]. Metals, particularly Ni, have been employed as a main component of cermets, such as Al_2O_3/Ni [6] and WC/Ni [12], due to its good sinterability, high oxidation resistance and ductibility. However, no study about the effect of Ni addition on the sintering behavior of hBN has been reported.

Common mechanical mixing of hBN powder and a small amount of Ni powder would not yield uniform distribution because of their different mechanochemical characteristics. Therefore, direct deposition of Ni nanoparticles on hBN powder could be promising for uniform mixing of Ni additive in hBN powder. Coating and precipitation on the surface of powder have been conducted by several methods including sol–gel and chemical vapor depoisition (CVD) [13,14]. Fluidized bed CVD (FBCVD), in particular, has been widely employed for coating on powders. However, the application of FBCVD on powder is limited depending mainly on density and particle size of powder. The use of a rotary CVD (RCVD) to prepare TiN coated titanium, graphite and iron powders has been reported [15,16]. This method can be applied to wide variety of powders without limitation of density and size of powders. However, there have been no reports of attempts to prepare metal nanoparticles as a sintering additive on ceramic powders. In this study, Ni nanoparticles have been prepared on hBN powder by RCVD, and the sintering behavior of the powder has been studied by spark plasma sintering (SPS).

2. Experimental procedure

Ni nanoparticles were precipitated on hBN powder by RCVD using nickelocene ($NiCp_2$) as a precursor. Fig. 1 shows a schematic of the RCVD apparatus, mainly consisting of a precursor evaporator and a reactor. Four alumina blades were attached to the inner wall of the alumina reactor to suspend hBN powder in a space by rotating the reactor in order to increase the contact time of the reactant gas and powder. The $NiCp_2$ precursor in the evaporator was heated at 393–423 K, and carried into the reaction zone by H_2 under a flow rate of 1.67×10^{-6} m^3 s^{-1}. The supply rate (R_s) of $NiCp_2$ was varied from 0 to 1.12×10^{-6} kg s^{-1}. The hBN powder (approx. 2–4 μm in grain size) was fed into the reactor and preheated at 793–823 K. The total

* Corresponding author.
E-mail address: goto@imr.tohoku.ac.jp (T. Goto).

0925-8388/$ – see front matter © 2010 Elsevier B.V. All rights reserved.
doi:10.1016/j.jallcom.2010.04.170

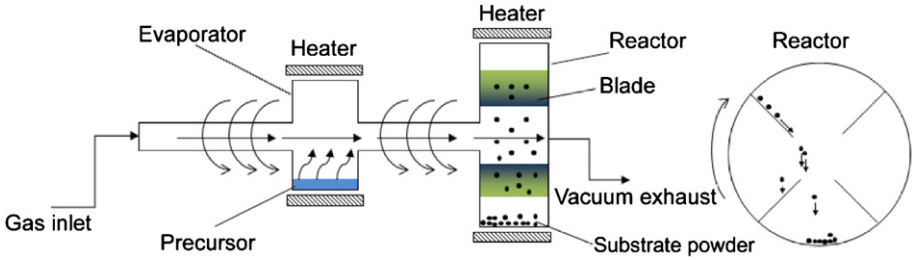

Fig. 1. Schematic of rotary CVD.

pressure of the RCVD apparatus was kept at 800 Pa. The deposition time was fixed at 1.8 ks.

The Ni nanoparticle precipitated hBN (hereafter Ni/hBN) powder was consolidated by spark plasma sintering (SPS, model SPS-210LX, SPS Syntex Inc., Japan). The sintering temperature ranged from 1773 to 2273 K. The heating rate was 3.3 K s^{-1}, and the sintering time was 0.6 ks. A pressure of 100 MPa was loaded from the beginning of the sintering process. The temperature was measured by an optical pyrometer focused on a hole (Φ2 mm × 5 mm) in the graphite die.

The crystal structure and phase of the Ni/hBN powder and the sintered bodies were identified by X-ray diffraction (XRD) with CuKα radiation. The microstructure was observed by scanning electron microscopy (SEM) and transmission electron microscopy (TEM). The average grain size of the Ni nanoparticles was calculated from 50 particles in the TEM images. The Ni content (CNi) in the Ni/hBN powder was estimated by energy-dispersive X-ray spectroscopy (EDS) and was averaged by five measurements at different areas. The bulk density of the sintered body was determined by an Archimedes' method and converted to relative density using the theoretical density of hBN (2.28×10^3 kg m^{-3}) [17] and Ni (8.91×10^3 kg m^{-3}) [18]. Vickers hardness (Hv) at room temperature was evaluated by a Vickers microhardness tester (HM-221, Mitutoyo Corp.) under a load (P) of 0.098 N, and was averaged by ten points.

3. Results and discussion

Fig. 2 shows the effects of precursor supply rate (R_s) on XRD patterns of the Ni/hBN powders. The diffraction peaks at $2\theta = 43.2°$(1 1 1), 50.3°(2 0 0), and 74.1°(2 2 0) were indexed to Ni, and no NiO and C peaks were identified. With increasing R_s, the intensities of Ni peaks increased, indicating the increase of the Ni content. Fig. 3 demonstrates the effect of R_s on the Ni content estimated from EDS. The Ni content increased up to 4 mass%, showing an almost linear relation between R_s and Ni content.

Fig. 4 shows the nano-structure of Ni particles precipitated on hBN powders at various R_s. Fine Ni particles less than 10 nm in size were partly precipitated on the flake-like hBN powder at $R_s = 0.28 \times 10^{-6}$ kg s^{-1} (Fig. 4(a)). The Ni particles were preferentially precipitated at the edge of hBN flakes (Fig. 4(b)). At $R_s = 0.56 \times 10^{-6}$ kg s^{-1}, Ni particles about 10 nm in size were distributed uniformly on the hBN surface (Fig. 4(c and d)). At $R_s = 0.84$ to 1.12×10^{-6} kg s^{-1}, the Ni powders grew to several 10 nm and agglomerated (Fig. 4(e–h)). The effect of R_s on the Ni particle size was shown in Fig. 5. The average grain size of Ni particles increased to about 80 nm gradually with increasing R_s to 1.12×10^{-6} kg s^{-1}. The size distribution range also increased with R_s.

Fig. 6 shows the relative density of the hBN bodies using the Ni/hBN powder with various Ni contents sintered at 2073 K. The relative density of the hBN bodies increased from 92 to 96% with increasing Ni content up to 1.87 mass% and then slightly decreased. Fig. 7(a) and (b) shows the microstructure of hBN bodies without and with Ni sintered at 2073 K, respectively. The white particles were identified as the Ni phase, and the gray matrix phase was hBN. In the hBN body without Ni, some pores and cleavages were observed (Fig. 8(a)). The pores in the hBN body with Ni (C_{Ni} = 1.87 mass%) decreased (Fig. 8(b)).

Fig. 8 shows the relative density of hBN bodies with Ni (C_{Ni} = 1.87 mass%) and sintered at 1773–2273 K in comparison with hBN bodies. The relative density of hBN bodies with Ni increased with increasing sintering temperature and showed the highest value of 97.3% at 2273 K, while those of hBN bodies without Ni were about 5% lower than those of hBN bodies with Ni. Fig. 9 (a) and (b)

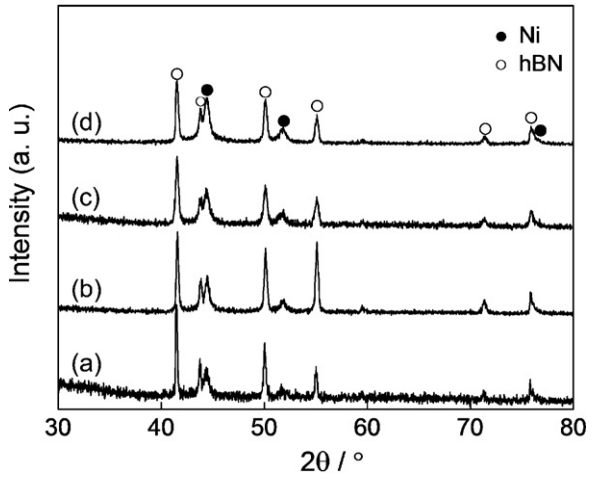

Fig. 2. X-ray diffraction (XRD) patterns of Ni-coated powders (a) $R_s = 0.28 \times 10^{-6}$ kg s^{-1}, (b) $R_s = 0.56 \times 10^{-6}$ kg s^{-1}, (c) $R_s = 0.84 \times 10^{-6}$ kg s^{-1}, and (d) $R_s = 1.12 \times 10^{-6}$ kg s^{-1}.

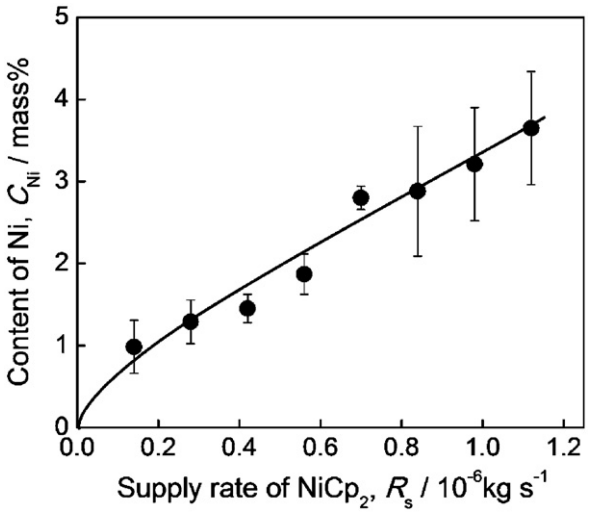

Fig. 3. Relationship between the Ni content and R_s.

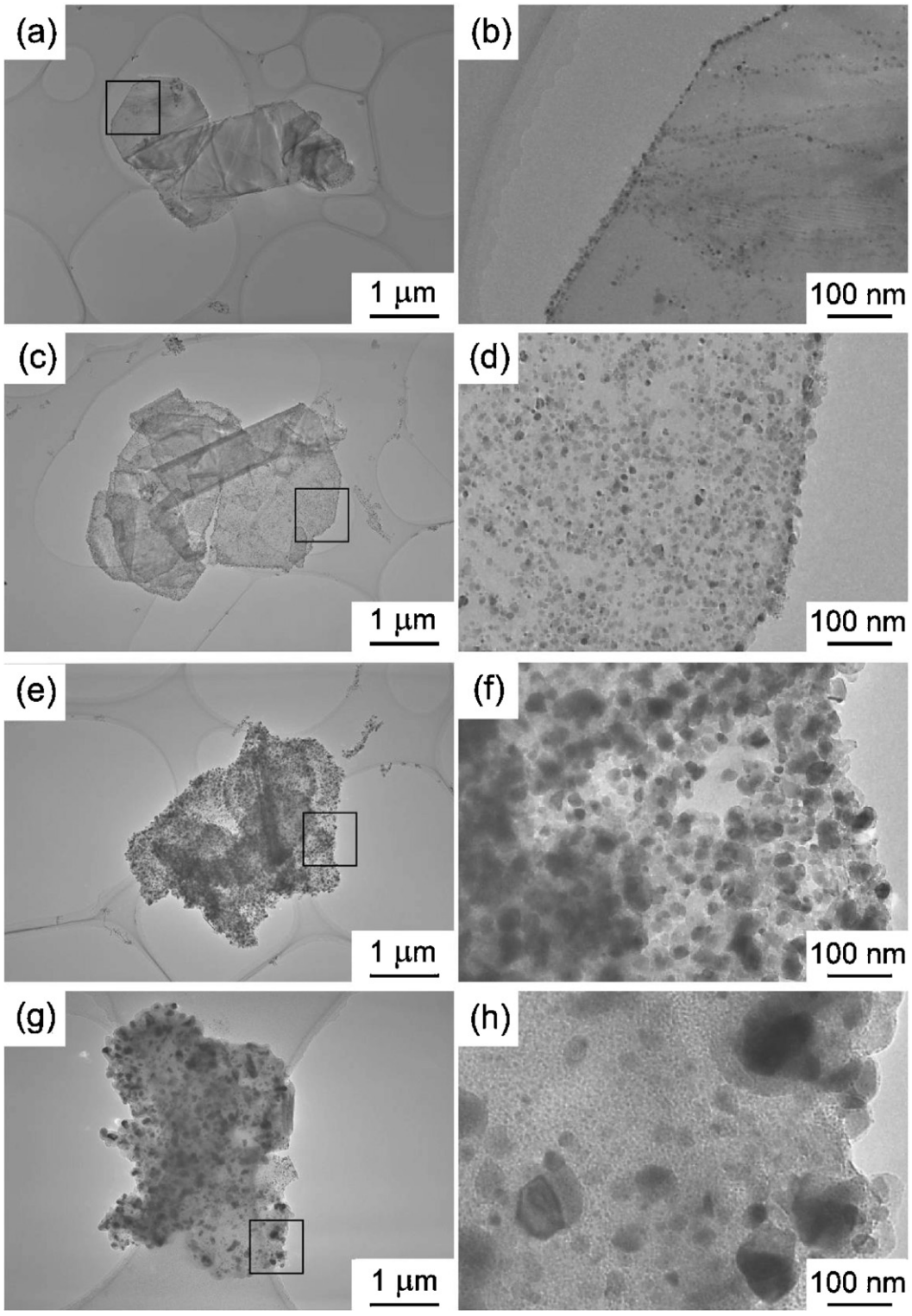

Fig. 4. Effect of R_s on morphology of Ni nanoparticles precipitated hBN powders (a) $R_s = 0.28 \times 10^{-6}$ kg s^{-1}, (b) $R_s = 0.28 \times 10^{-6}$ kg s^{-1}, high magnification of (a), (c) $R_s = 0.56 \times 10^{-6}$ kg s^{-1}, (d) $R_s = 0.56 \times 10^{-6}$ kg s^{-1}, high magnification of (c), (e) $R_s = 0.84 \times 10^{-6}$ kg s^{-1}, (f) $R_s = 0.84 \times 10^{-6}$ kg s^{-1}, high magnification of (e), (g) $R_s = 1.12 \times 10^{-6}$ kg s^{-1}, and (h) $R_s = 1.12 \times 10^{-6}$ kg s^{-1}, high magnification of (g).

Table 1
Literature data on hBN bodies by sintering.

	Hagio et al. [3,4].	Kurita et al. [19]	Höhn and Obenaus [20]	This work	This work
Additive	B_2O_3	AlN, active B	B_2O_3	No additive	Ni
Sintering method	Pressureless sintering	Pressureless sintering	Hot pressing	SPS	SPS
Atmosphere	Flowing Ar	N_2	–	Vacuum	Vacuum
Sintering temperature	2273 K	1773 K	–	2273 K	2273 K
Holding time	1 h	–	–	10 min	10 min
Relative density	<80%	75.8%	94%	95.1%	97.3%

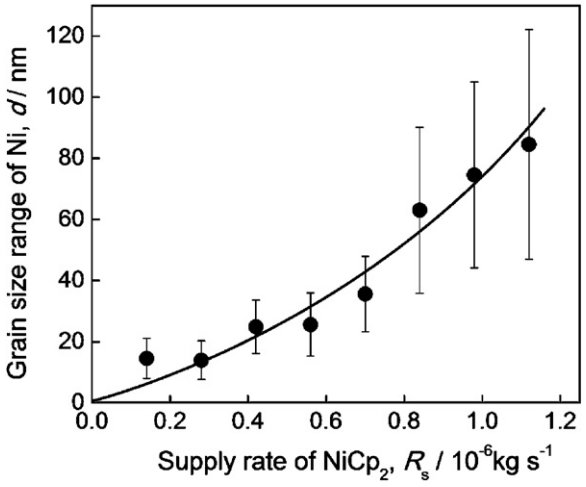

Fig. 5. Grain size distribution of Ni particles distributed on hBN powder surface.

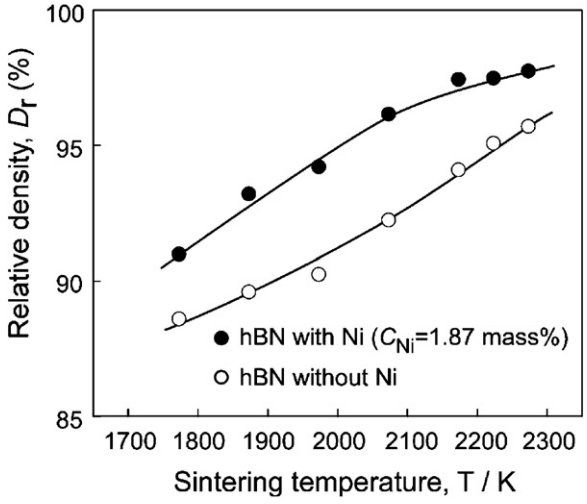

Fig. 8. Effect of sintering temperature on the relative density of the hBN bodies using hBN powders without and with Ni.

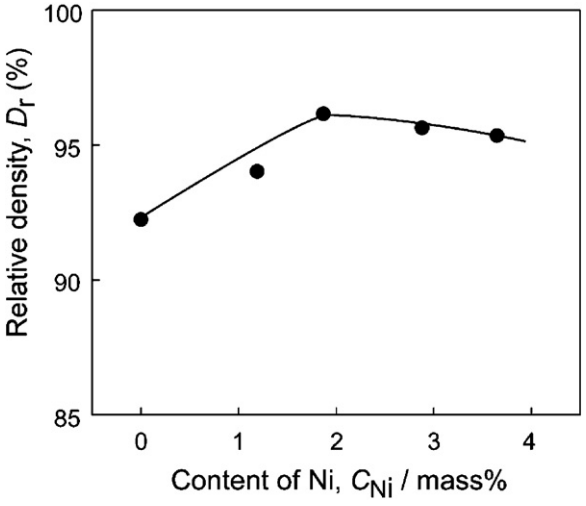

Fig. 6. Effect of Ni content (C_{Ni}) on the relative density of the samples sintered from Ni-coated and uncoated hBN powders.

shows the microstructure of the hBN body without and with Ni, respectively. The hBN body with Ni was denser than that without Ni, and the amount of Ni decreased probably due to partial evaporation at high temperatures. Fig. 10 shows the Vickers hardness (H_v) of hBN bodies with Ni (C_{Ni} = 1.87 mass%) sintered at 1873–2273 K in comparison with hBN bodies. Both of the H_v of the hBN without and with Ni increased with increasing sintering temperature. The H_v of the hBN body with 1.87 mass% Ni was almost two times that of the hBN bodies without Ni, showing the highest value of about 0.3 GPa.

Table 1 shows a comparison of our work with reports in literature on sintered hBN bodies [3,4,19,20]. Kurit et al. consolidated a hBN body at 1773 K in N_2 by pressureless sintering using AlN and active B as sintering additives, where the relative density was 75.8%. Hagio et al. used B_2O_3 as a sintering additive by pressureless sintering, the relative density being <80% at 2237 K for 1 h. Höhn et al. also used B_2O_3 as a sintering additive by hot pressing and obtained a relative density of 94%. In this work, the relative density of the hBN body with Ni (C_{Ni} = 1.87 mass%) reached 97.3% as shown by SPS. This value was the highest thus far reported for a hBN body.

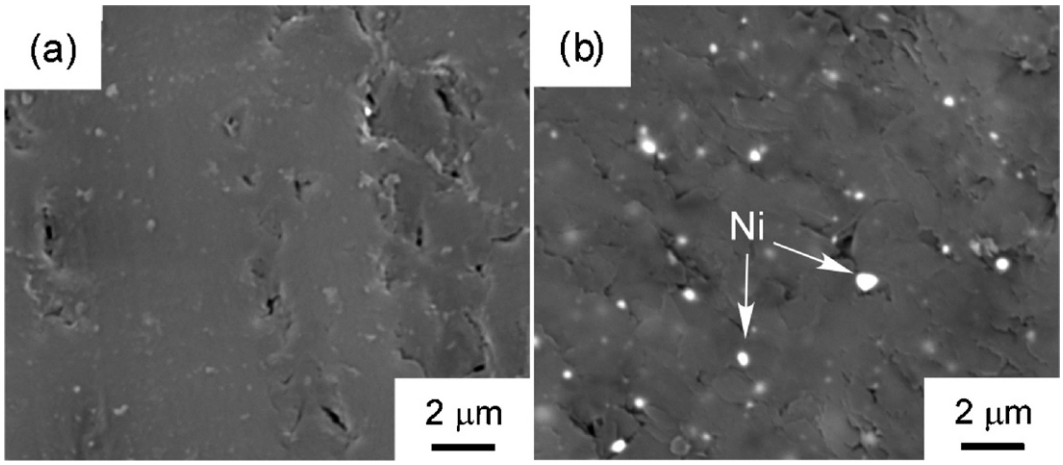

Fig. 7. Back-scattered SEM images of the hBN bodies without (a) and with Ni (C_{Ni} = 1.87 mass%) (b) sintered at 2073 K.

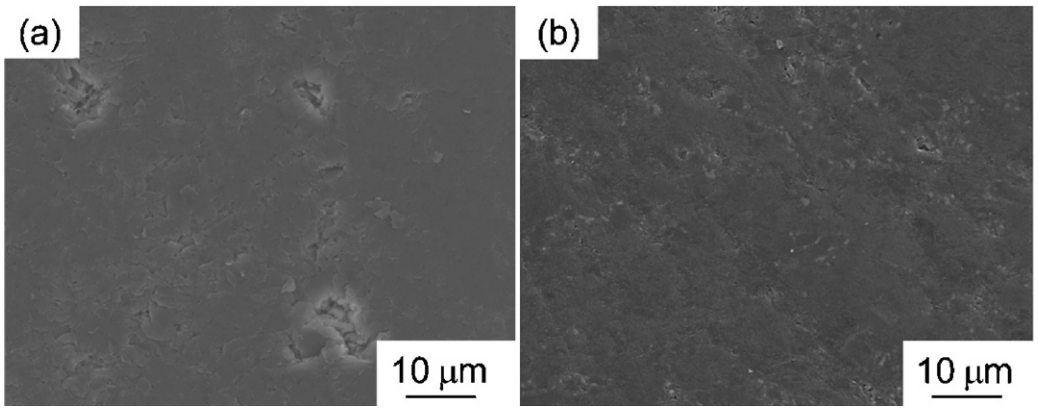

Fig. 9. SEM images of hBN bodies without (a) and with Ni (C_{Ni} = 1.87 mass%) (b) sintered at 2273 K.

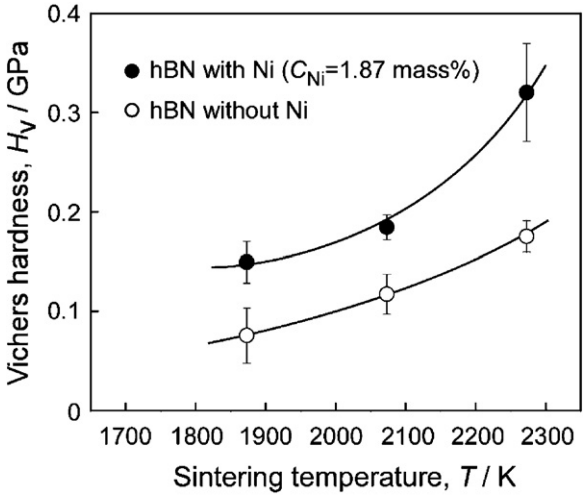

Fig. 10. Vickers hardness of hBN bodies without and with Ni (C_{Ni} = 1.87 mass%) sintered at 1873–2273 K.

4. Conclusion

Ni nanoparticles were precipitated on hBN powders by rotary chemical vapor deposition. The grain size and content of Ni increased from 13.9 to 84.5 nm and 0.98 to 3.65 mass%, respectively, with increasing supply rate of $NiCp_2$ from 0 to 1.12 mass%. The Ni nanoparticles enhanced the densification of hBN body by SPS. The highest relative density of hBN body was 97.3% at 2273 K.

Acknowledgements

This research was financially supported by the Rare Metal Substitute Materials Development Project, New Energy and Industry Technology Development Organization (NEDO), by the Global COE Program "Materials Integration (International Center of Education and Research), Tohoku University", and by the International Collaboration Center, ICC-IMR, Tohoku University.

References

[1] A. Lipp, K.A. Schwetz, K. Hunold, J. Eur. Ceram. Soc. 5 (1989) 3–9.
[2] J. Eichler, C. Lesniak, J. Eur. Ceram. Soc. 28 (2008) 1105–1109.
[3] T. Hagio, H. Yoshida, J. Mater. Sci. Lett. 13 (1994) 653–655.
[4] T. Hagio, K. Kobayashi, H. Yasunaga, H. Nishikawa, J. Am. Ceram. Soc. 72 (1989) 1482–1484.
[5] D. Belforti, Nature 190 (1961), 901.
[6] J.S. Lu, L. Gao, L.H. Gui, J.K. Guo, Mater. Chem. Phys. 72 (2001) 352–355.
[7] Y. Ji, J.A. Yeomans, J. Eur. Ceram. Soc. 22 (2002) 1927–1936.
[8] M. Nawa, K. Yamazaki, T. Sekino, K. Niihara, J. Jpn. Soc. Powder. Powder. Metall. 41 (1994) 1220–1225.
[9] M. Nawa, K. Yamazaki, T. Sekino, K. Niihara, Mater. Lett. 20 (1994) 299–304.
[10] A.A. Khan, J.C. Labbe, J. Eur. Ceram. Soc. 16 (1996) 739–744.
[11] A.A. Khan, J.C. Labbe, J. Eur. Ceram. Soc. 17 (1997) 1885–1890.
[12] S. Imasato, K. Tokumoto, T. Kitada, S. Sakaguchi, Int. J. Refract. Met. H. 13 (1995) 305–312.
[13] A. Boulle, Z. Oudjedi, R. Guinebretière, B. Soulestin, A. Dauger, Acta. Mater. 49 (2001) 811–816.
[14] G. Vahlas, B. Caussat, P. Serp, G.N. Angelopoulos, Mater. Sci. Eng. R 53 (2006) 1–72.
[15] H. Itoh, N. Watanabe, S. Naka, J. Mater. Sci. 23 (1988) 43–47.
[16] H. Itoh, K. Hattori, S. Naka, J. Mater. Sci. 24 (1989) 3643–3646.
[17] JCPDS, International Centre for Diffraction Data, No. 34-0421.
[18] JCPDS, International Centre for Diffraction Data, No. 04-0850.
[19] S. Kurita, M. Nakashima, H. Takape, J. Min. Mater. Process. Inst. Jpn. 105 (1989) 201–204.
[20] S. Höhn, P. Obenaus, Pract. Metall. 36 (2004) 299–301.